

# Ising spin glasses: Corrections to finite size scaling, freezing temperatures, and critical exponents

P. O. Mari and I. A. Campbell

*Laboratoire de Physique des Solides, Université Paris Sud, 91405 Orsay, France*

(Received 23 June 1998; revised manuscript received 1 October 1998)

We compare simulation data from different sources on two canonical three-dimensional Ising spin glasses (ISGs): the binomial  $\pm J$  near-neighbor interaction ISG and the Gaussian interaction ISG. We allow for the possibility of corrections to finite size scaling and estimate the correction exponent  $w$ . Consistent estimates for the critical temperatures  $T_g$  and for the critical exponents for each system are obtained. The data strongly indicate that critical exponents in the two systems are significantly different from each other. These results thus confirm a breakdown of standard universality rules in Ising spin glasses. [S1063-651X(99)01503-2]

PACS number(s): 05.50.+q, 75.50.Lk, 64.60.Cn, 75.40.Cx

## I. INTRODUCTION

The values for the universal exponents at canonical second-order transitions are well established [1]; recent work has only modified very slightly the accurate estimates for the dimension-3 exponents [2]. In contrast, for spin glass models accurate values of the freezing temperature  $T_g$  and *a fortiori* of the critical exponents have been very difficult to estimate numerically because of the intrinsic slow dynamics close to the transition.

Large-scale dynamic simulations on the 3d Ising spin glass (ISG) with binomial  $\pm J$  near-neighbor interactions by Ogielski [3] led to estimates of  $T_g$  and the whole set of static and dynamic exponents. Recently extensive simulation data analyzed using finite size scaling have been reported on the same system [4]. The authors relied principally on the Binder cumulant method to evaluate  $T_g$  and estimated a significantly lower value than that of Ogielski. However, a different scaling method [5] led to a value agreeing with the Ogielski estimate. Simulations have also been carried out on the 3d ISG with Gaussian interactions [6,5].

We have reviewed the data in order to establish if and when correction terms should be included in the finite size scaling analyses, and we try to obtain a consistent overall interpretation. Our final aim is to check our earlier statement [5,7] that critical parameters vary between systems with different sets of interactions, meaning that conventional universality does not hold in ISGs.

## II. SCALING RELATIONS

We will first recall scaling relations which will be used in the analysis [8]. At a given size and temperature, the equilibrium spin glass susceptibility is related to the second moment of the fluctuations of the autocorrelation function  $q(t)$  through

$$\chi_{SG} = L^d \langle q^2 \rangle \quad (1)$$

( $L$  is the linear size of the system and  $d$  is its dimension) and its standard finite size scaling (FSS) formula is

$$\chi_{SG} = L^{2-\eta} f(L^{1/\nu}(T-T_g)). \quad (2)$$

$T_g$ ,  $\eta$ , and  $\nu$  can be estimated from a scaling plot. Right at  $T_g$  for dimension 3 we should find

$$L \langle q^2 \rangle \propto L^{-\eta} \quad (3)$$

and therefore a linear relation on a log-log plot.

The Binder cumulant is defined by

$$g_L = \frac{1}{2} \left( 3 - \frac{\langle q^4 \rangle}{\langle q^2 \rangle^2} \right). \quad (4)$$

Binder plots for fixed  $L$  should all intersect at  $T_g$  and the Binder cumulant values should follow a scaling form

$$g_L = g(L^{1/\nu}(T-T_g)). \quad (5)$$

However, Eqs. (1)–(5) ignore possible corrections to FSS. When these are included, the expression for the spin glass susceptibility becomes

$$\chi_{SG} = L^{2-\eta} f(L^{1/\nu}(T-T_g)) \times [1 - L^{-w} f_L(L^{1/\nu}(T-T_g))] + O(L^{-2w}) \quad (6)$$

and there is a similar expression for  $\langle q^4 \rangle$ . At small sizes,  $g_L$  will be modified through the corrections to both  $\langle q^2 \rangle$  and  $\langle q^4 \rangle$ . For the 3d Ising ferromagnet, the correction to the scaling exponent  $w$  is  $0.87 \pm 0.09$ , while for the 3d site percolation problem  $w$  is  $1.62 \pm 0.13$  [9]. High values of  $w$  imply that deviations from scaling drop rapidly as  $L$  increases; however, it has been suggested that when  $w$  is large, subleading terms can be expected to play a role also [9,10]. Up to now, the exponent  $w$  has not been estimated numerically for ISGs.

We can also obtain independent estimates of  $T_g$ ,  $\eta$ , and  $z$  using the method introduced by Bernardi *et al.* [5,7]. First, as the ISG is quenched from an infinite temperature configuration to  $T_g$ , the spin glass susceptibility increases with time as  $t^h$  with [11,12]

$$h = \frac{2-\eta}{z}. \quad (7)$$

Second, if we measure the decay of the autocorrelation function  $q(t)$  for a well annealed sample at  $T_g$  the initial decay with time is as  $t^{-x}$  with [3]

$$x = \frac{d-2+\eta}{2z}. \quad (8)$$

Combining these measurements at a set of test temperatures near  $T_g$  gives us a first set of effective values  $\eta_1(T)$ . Independently, the equilibrium spin glass susceptibility as a function of sample size  $L$  at  $T$  near  $T_g$  gives us another set of effective values  $\eta_2(T)$ . Consistency dictates that the true  $T_g$  and  $\eta$  must correspond to the intersection point of the two independent  $\eta(T)$  plots. This method allows us to estimate  $T_g$ ,  $\eta$ , and  $z$ .

We can comment on the practical application of these methods. First, a scaling plot for  $\chi$  has three free parameters ( $T_g$ ,  $\eta$ , and  $\nu$ ). If the scaling is poor for a given set, then that set can be ruled out; on the other hand, two different sets may give equally good scaling so the method is not always discriminatory. The Binder cumulant technique should in principle lead to a clear value of  $T_g$ ; however, for the particular case of  $3d$  ISGs, the Binder cumulant curves near the estimated  $T_g$  lie very close together [4,6], so any residual statistical errors or corrections to FSS can have a drastic effect on the precise position of the crossing points between the curves.

The  $\eta_1(T)$  in the Bernardi *et al.* method is obtained using large samples and so should not be subject to finite size corrections.

### III. 3D BINOMIAL $\pm J$ ISG MODEL

We will now discuss the binomial case. Ising spins on a simple cubic lattice are coupled through random binomial ( $\pm J$ ) near-neighbor interactions. Ogielski [3] carried out dynamic simulations on samples with  $L$  up to 64. From the divergence of the susceptibility and relaxation time he estimated  $T_g = 1.175 \pm 0.025$ . Bernardi *et al.* [5] obtained a scaling value for  $T_g$  in agreement with Ogielski. Kawashima and Young [4] carried out very high quality numerical measurements down to  $T=0.96$  for sample sizes  $L$  from 6 to 16 and down to  $T=1.195$  for  $L=24$ . They measured the moments of the equilibrium fluctuations of the autocorrelation function,  $\langle q^2 \rangle$  and  $\langle q^4 \rangle$ . From the estimated intersection point of the raw Binder cumulant curves, they deduced a value for  $T_g = 1.11 \pm 0.04$ . With this value of  $T_g$  in hand and the scaling relations, they further estimated the critical exponents. They have generously put their spin glass susceptibility data at our disposal. We have completed their series of data with measurements taken at the same temperatures and with smaller sizes,  $L=3$  and  $L=4$ . Kawashima and Young [4] pointed out that their data could be subject to corrections to finite size scaling, as their scalings for the Binder parameter and for  $\langle q^2 \rangle$  did not lead to fully consistent estimates for  $\nu$ .

We will proceed by steps, starting with the  $\langle q^2 \rangle$  data rather than the Binder cumulant. First, if we accept the parameter set  $[T_g, \eta, \nu]$  quoted in Ref. [4], i.e.,  $[1.11, -0.35, 1.7]$ , the  $\langle q^2 \rangle$  data for  $L=6$  to  $L=24$  lead to the scaling plot in Fig. 1. If we choose instead the parameter set

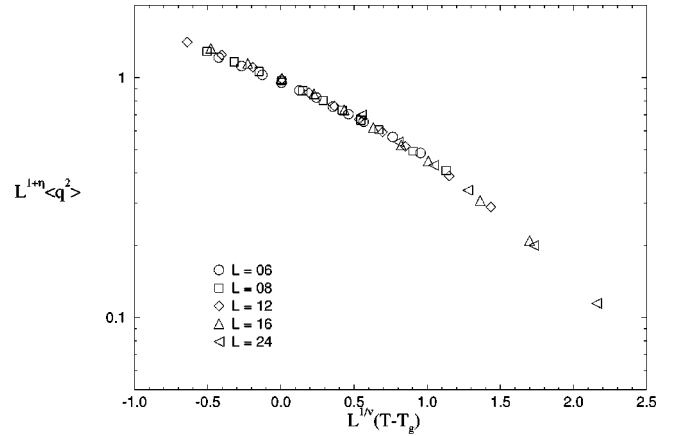


FIG. 1. Scaling plot of  $\langle q^2 \rangle$  with  $T_g = 1.11$ ,  $\eta = -0.35$ , and  $\nu = 1.7$  for the  $\pm J$  Ising spin glass model [4].

$[1.19, -0.22, 1.33]$ , consistent with [3,5], we find equally good scaling, Fig. 2.

If we now plot  $\log_{10}(L \langle q^2 \rangle)$  against  $\log_{10}(L)$  at the temperature 1.195 including results for  $L=3$  and 4, the data show a bend at small  $L$  and a straight line at large  $L$ , Fig. 3. This is consistent with a  $T_g$  close to 1.195 together with corrections to FSS for smaller sizes. In fact, similar down bending can be seen at the other temperatures as well when the data are plotted in this way. The effect is clearest at  $T = 1.195$  as this is the lowest temperature where data extend to  $L=24$ , giving a good estimate of the large size limiting behavior. Assuming that only the leading term in the correction to finite size scaling is important, we can fit the points with Eq. (6) ignoring the  $O(L^{-2w})$  term and replacing the function  $f_L$  by a constant  $k$ . The curve in Fig. 3 corresponds to  $\eta = -0.22$  and  $w = 2.8$ . If we make the approximation that, in the range of temperatures covered by the simulations, the correction factor is temperature independent (i.e., we set the correction scaling function  $f_L$  to  $k$  everywhere as otherwise we would have too many uncontrollable free parameters), we can generate a set of ‘‘corrected’’  $\langle q^2 \rangle$  values for all the  $L$  and  $T$ :

$$\langle q^2 \rangle^* = \frac{\langle q^2 \rangle}{1 - kL^{-w}}. \quad (9)$$

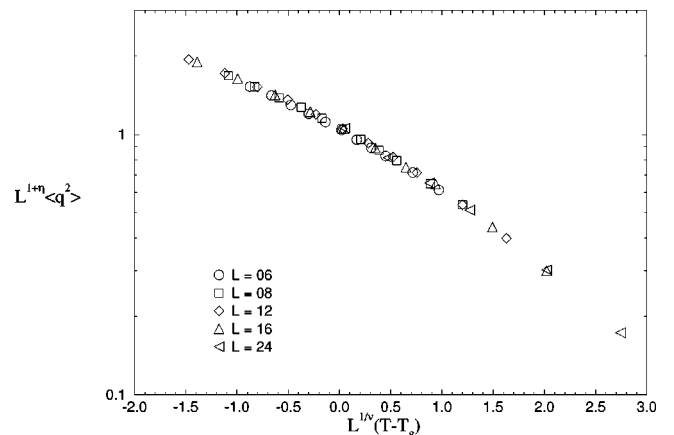


FIG. 2. Same type of scaling plot as in Fig. 1, but with  $T_g = 1.19$ ,  $\eta = -0.22$ , and  $\nu = 1.33$ .

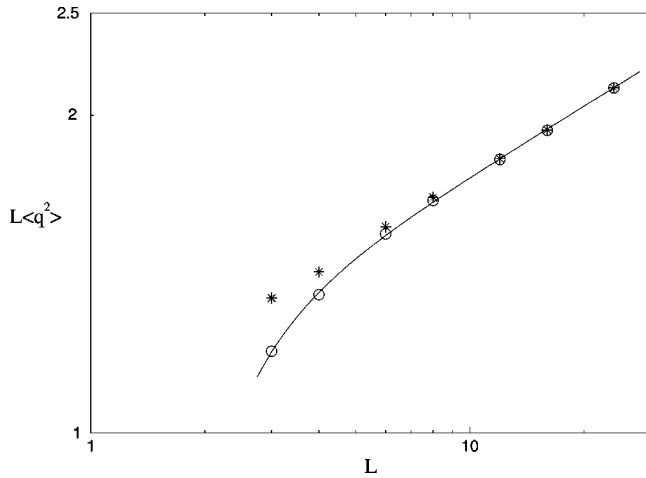


FIG. 3.  $L\langle q^2 \rangle$  versus  $L$  plot for the raw  $\pm J$  ISG data [4] (circles) with its corresponding fit (line) ( $\eta = -0.22$  and  $w = 2.8$ ) taking into account the finite size scaling corrections [Eq. (6)]. The stars mark the “corrected”  $L\langle q^2 \rangle$  data. This figure clearly shows that the corrections to FSS are still present at sizes up to  $L = 8$ .

We can now make a new scaling plot, Fig. 4, using the corrected  $\langle q^2 \rangle^*$  values. With the same scaling parameter set [ $T_g$ ,  $\eta$ , and  $\nu$ ] as before, the new scaling plot (Fig. 4) is now of excellent quality, implying that the analysis is self-consistent.

The large value of  $w$  is entirely consistent with quite independent series results on the  $\pm J$  ISG [13]. In the series work, corrections to scaling are represented by the parameter  $\Delta_1$ , where  $\Delta_1 = w\nu$ . The series results lead to ( $\Delta_1 \sim 3$ ) in  $4d$  and ( $\Delta_1 \sim 4$ ) in  $3d$  (it is expected that  $\Delta_1$  gets larger as the dimension decreases below the upper critical dimension [13,14]). Thus in  $3d$ , the series result  $\Delta_1 \sim 4$  and the present simulation result  $w\nu \sim 3.7$  are entirely consistent.

From new simulations we have obtained more accurate data for the effective values of the Huse parameter  $h(T)$  as a function of temperature in the region near  $T_g$ . Combining these  $h(T)$  values with the effective power-law relaxation exponent values  $x(T)$  from Ogielski’s relaxation work [3], we obtain a first set of effective values  $\eta_1(T)$ . We obtain a

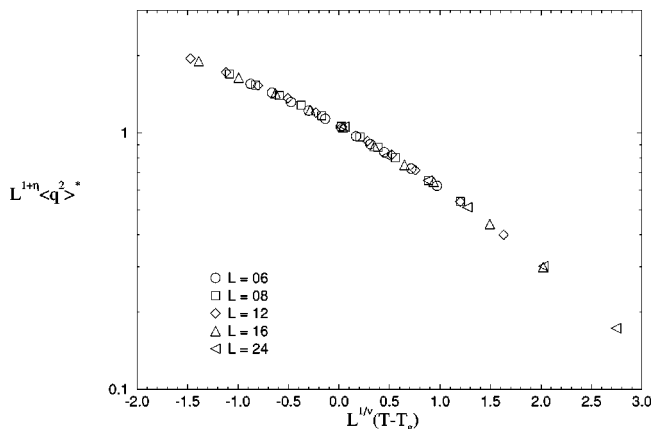


FIG. 4. Scaling plot of the corrected data of Fig. 2 ( $\langle q^2 \rangle^*$ ) with  $T_g = 1.19$ ,  $\eta = -0.22$ , and  $\nu = 1.33$ . The quality of the FSS plot has improved and is not degraded if we include sizes  $L = 3$  and  $4$ .

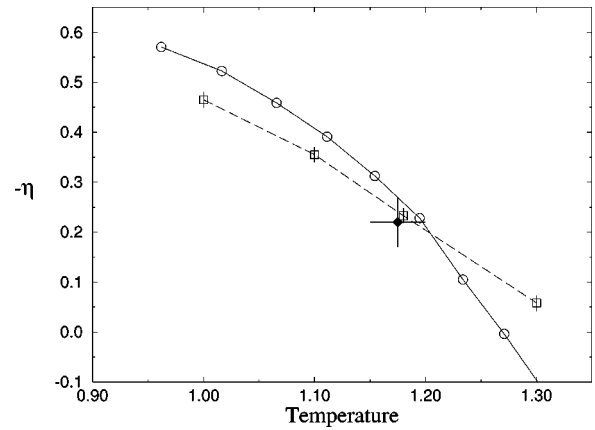


FIG. 5.  $\eta_1(T)$  (squares) and  $\eta_2(T)$  from [4] (circles) versus temperature for the  $\pm J$  ISG model. According to [5], the intersection point between the two  $\eta(T)$  curves gives an estimate of  $T_g$  and  $\eta$ : we obtained  $T_g = 1.20 \pm 0.01$  and  $\eta = -0.21 \pm 0.02$ . This figure also includes another estimate of  $\eta$  and  $T_g$  from [3], full diamond.

second set of  $\eta_2(T)$  from the slopes of the  $\log_{10}(L\langle q^2 \rangle)$  against  $\log_{10}(L)$  plots at large  $L$  (the data of [4]), Fig. 5. The intersection point between the two  $\eta(T)$  curves gives us  $T_g = 1.20 \pm 0.01$  and  $\eta = -0.21 \pm 0.02$ . Thus the two independent estimates of  $T_g$  and  $\eta$ , from Ogielski’s dynamic data, and from the Bernardi *et al.* method, are in good agreement. The  $\langle q^2 \rangle$  scaling of Fig. 4 is also consistent with this analysis.

What about the Binder cumulants? Like  $\langle q^2 \rangle$ ,  $\langle q^4 \rangle$  values are also subject to corrections to FSS. Figure 6 shows the  $L^2\langle q^4 \rangle$  data as a function of  $L$  again at the temperature 1.195. The curve is a fit of the same form as for the equivalent  $L\langle q^2 \rangle$  plot. The fit parameters are a high  $L$  slope of 0.44 (equal to  $-2\eta$  if we are at  $T_g$ ) and  $w = 2.0$ . We can note that the two fitting values of  $w$  for  $\langle q^2 \rangle$  and for  $\langle q^4 \rangle$  are not identical whereas scaling theory tells us that they should be the same. However, the  $w$  exponents we are quoting are only “effective” exponents; as was pointed out [9], when  $w$  is high, subleading terms cannot be ignored. We surmise that the true leading term value of  $w$  is close to 2.8, but that the  $\langle q^4 \rangle$  is affected by subleading terms so the apparent value of  $w$  appears a little different. We have used the fit curves of Figs. 3 and 6 as providing empirical size-dependent correc-

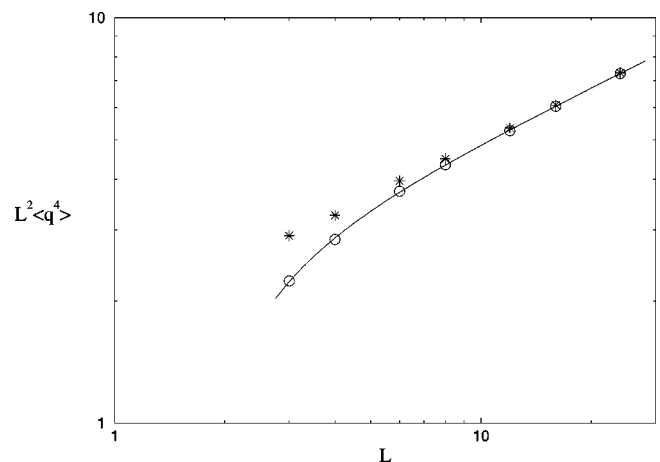


FIG. 6. Same type of plot as in Fig. 3, but with the raw  $L^2\langle q^4 \rangle$  data [4]. Here,  $\eta = -0.44$  and  $w = 2.0$ .

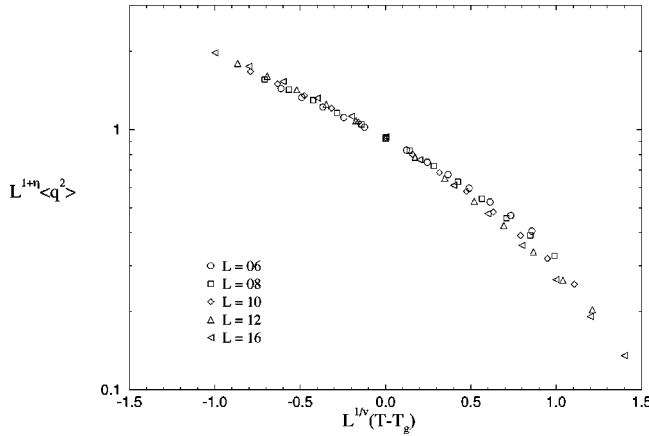


FIG. 7. Scaling plot of  $\langle q^2 \rangle$  with  $T_g = 0.95$ ,  $\eta = -0.36$ , and  $\nu = 2.0$  for the 3d Gaussian Ising spin glass model [6].

tion factors for the range of  $L$  studied. With corrected  $\langle q^4 \rangle$  and  $\langle q^2 \rangle$  values we can generate a set of corrected Binder cumulant values. The corrected Binder cumulant curves all intersect near  $T = 1.19$ .

We are not suggesting that this is a water-tight procedure for estimating  $T_g$  accurately. The point is that the data clearly show that there are correction terms present. A plausible procedure for allowing for corrections modifies the apparent ‘‘Binder’’  $T_g$ . But because Binder plots are highly sensitive to the precise correction terms, alternative techniques should be preferred for estimating  $T_g$  when correction terms are present. In fact, without going into the procedure we have just outlined, a simple qualitative check on the correct Binder cumulant intersection point can be obtained by concentrating attention on the raw  $g_L(T)$  curves for  $L = 16$  and  $L = 24$ , Fig. 2 of Ref. [4]. As these are the largest sizes, the curves should be the least affected by corrections to FSS. Already in the raw data [4] the intersection point of the two  $g_L(T)$  curves for these two sizes was at a temperature of about  $T = 1.195$ , indicating that this temperature is close to  $T_g$ .

#### IV. 3D GAUSSIAN ISG MODEL

We now turn to the 3d ISG with Gaussian interactions. Early work suggested  $T_g = 0.9 \pm 0.1$  [8]. Bernardi *et al.* [5] estimated  $T_g = 0.88 \pm 0.05$ . Recent large-scale simulations on sizes 4 to 16 [6] were interpreted as showing  $T_g = 0.95 \pm 0.04$ ,  $\nu = 2.0$ , and  $\eta = -0.36 \pm 0.06$ . The authors have kindly provided us with their susceptibility data. We have completed the  $\langle q^2 \rangle$  data sets with results at  $L = 3$ . In the discussion we will follow the same series of steps as for the binomial case. An  $L \langle q^2 \rangle$  scaling plot with the parameter set  $[T_g, \nu, \eta]$  given by [6] is of poor quality, Fig. 7. With the parameter set  $[0.875, 1.65, -0.49]$  the quality of scaling is much improved, Fig. 8. This suggests that  $T_g$  is near 0.88. Direct log-log plots of  $L \langle q^2 \rangle$  against  $L$  give an excellent straight line at  $T = 0.90$  over the whole range of  $L$ , Fig. 9, while the plots are curved for high  $L$  at temperatures above this value. This shows that for this system,  $T_g$  is near or below 0.90, and that the corrections to FSS are indiscernible for  $\langle q^2 \rangle$ , much smaller in any case than in the binomial

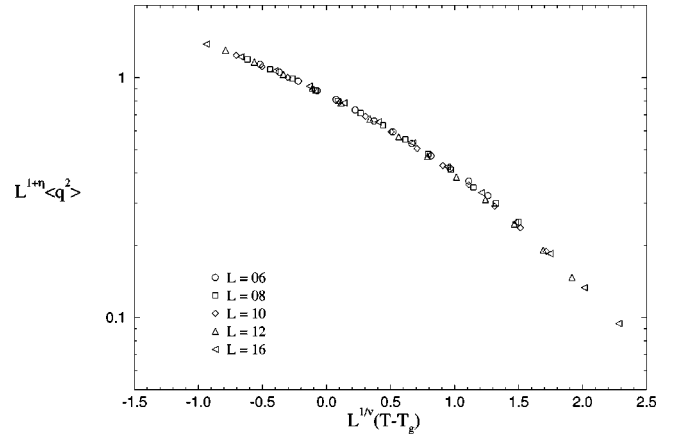


FIG. 8. Same type of scaling plot as in Fig. 7, but with an improved set of parameters:  $T_g = 0.875$ ,  $\eta = -0.49$ , and  $\nu = 1.65$ .

interaction system (compare Figs. 3 and 9).

Now having the Marinari *et al.*  $\langle q^2 \rangle$  data up to  $L = 16$  at hand [6], it is possible to give accurate values for the set of effective  $\eta_2(T)$  from  $\log_{10}(L \langle q^2 \rangle)$  against  $\log_{10}(L)$  plots. Hence the estimates for this system from the Bernardi *et al.* technique can be improved, Fig. 10. It can be seen that there is a clear intersection point corresponding to  $T_g, \eta$  equal to  $0.86 \pm 0.02, -0.51 \pm 0.02$ . The  $\langle q^2 \rangle$  scaling analysis and the Bernardi *et al.* technique give consistent results.

Finally we can examine the Binder cumulant data. A standard plot for  $g_L(T)$  with the data which can be read off the Marinari *et al.* plots [6] is shown in Fig. 11. The intersection of the curves occurs at  $T = 0.91 \pm 0.04$  giving a value of  $T_g$  which is essentially consistent with the  $L \langle q^2 \rangle$  scaling and the Bernardi *et al.* method.

#### V. COMPARISONS AND CONCLUSIONS

We can draw a first conclusion on the technical level. For systems like 3d ISGs where Binder cumulant plots for dif-

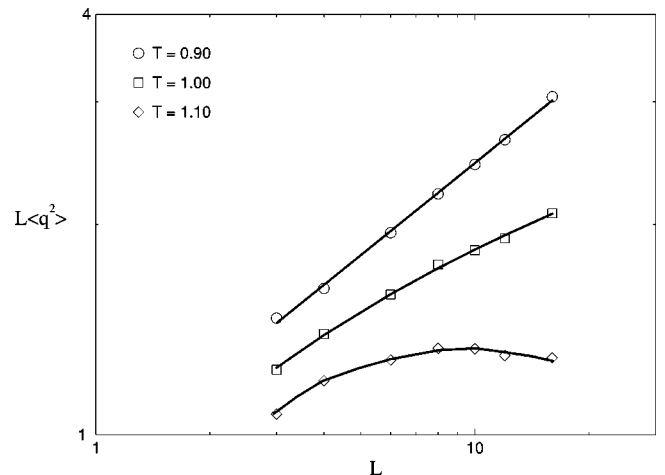


FIG. 9. Log-log plot of  $L \langle q^2 \rangle$  versus  $L$  for the raw Gaussian ISG data [6], at different temperatures close to  $T_g$ . The Gaussian ISG model exhibits no relevant corrections to FSS (compare Figs. 3 and 9). The lines are to guide the eye.

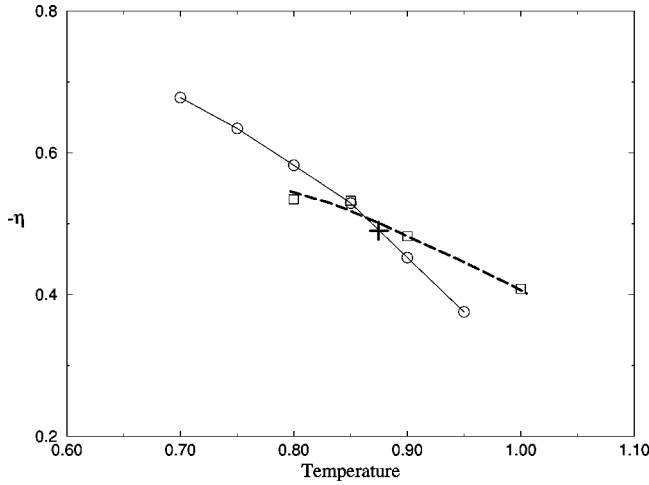


FIG. 10.  $\eta_1(T)$  (squares) and  $\eta_2(T)$  from [6] (circles) versus temperature for the Gaussian ISG model. The intersection point between the two  $\eta(T)$  curves gives  $T_g = 0.86 \pm 0.01$  and  $\eta = -0.51 \pm 0.02$ . This figure also includes (plus symbol) the estimate of  $\eta$  and  $T_g$  from the  $\langle q^2 \rangle$  scaling plot:  $T_g = 0.875 \pm 0.01$  and  $\eta = -0.49 \pm 0.02$ . The lines are to guide the eye.

ferent sizes lie very close together near  $T_g$ , and are sensitive to deviations from FSS and possibly other systematic problems, estimates of  $T_g$  from Binder cumulant curve intersections have to be treated with great caution. When accurate data to large  $L$  exist, scaling plots for  $\langle q^2 \rangle$  appear to be reliable as they are less sensitive to systematic errors, particularly to deviations from FSS. However, a scaling collapse may not be discriminatory as three parameters are involved. The method of Bernardi *et al.* [5], combining nonequilibrium scaling, dynamic scaling, and finite size scaling, is not sensitive to deviations from FSS and leads to precise and reliable estimates of  $T_g$  and the exponents. Once deviations from FSS are allowed for, the different methods appear to be consistent with each other.

Having gone through the procedure outlined above, we can summarize the conclusions concerning the corrections to

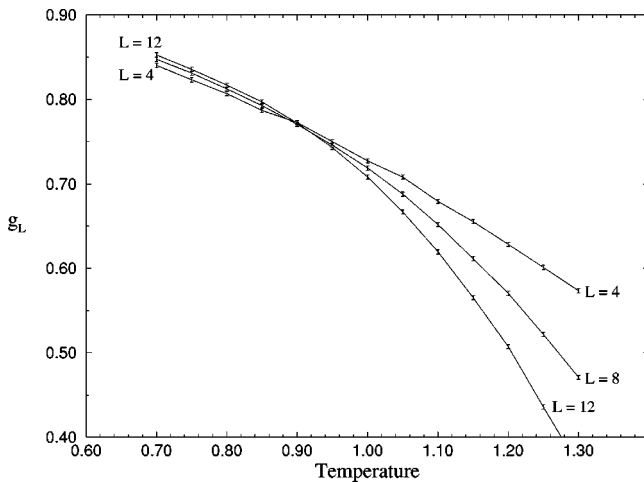


FIG. 11. Binder parameter  $g_L$  plotted against temperature for sizes  $L=4, 8,$  and  $12$  read off Marinari *et al.* [6] gives a clear intersection at  $T_g = 0.91 \pm 0.04$ . The error bars for  $L=16$  being much bigger, we have not included these points.

TABLE I. Estimates of  $T_g$ ,  $\eta$ , and  $\nu$  for the  $3d$  ISGs with binomial and Gaussian interactions using different techniques (see main body of text).

$\pm J$ ISG	$T_g$	$\eta$	$\nu$
Corrected FSS <sup>a</sup>	$1.19 \pm 0.01$	$-0.22 \pm 0.02$	$1.33 \pm 0.05$
Bernardi <i>et al.</i> method	$1.20 \pm 0.01$	$-0.21 \pm 0.02$	
Ogielski [3]	$1.175 \pm 0.025$	$-0.22 \pm 0.05$	$1.3 \pm 0.1$
Gaussian ISG	$T_g$	$\eta$	$\nu$
FSS <sup>b</sup>	$0.875 \pm 0.01$	$-0.49 \pm 0.02$	$1.65 \pm 0.05$
Bernardi <i>et al.</i> method	$0.86 \pm 0.01$	$-0.51 \pm 0.02$	

<sup>a</sup>Using  $\langle q^2 \rangle$  data from Ref. [4].

<sup>b</sup>Using  $\langle q^2 \rangle$  data from Ref. [6].

FSS, the ordering temperatures, and the various critical parameters for the canonical ISG systems with binomial and Gaussian interactions.

We estimate the correction to the FSS scaling exponent for the binomial ISG to be  $w \sim 2.8$  in good agreement with series results [13]. For the Gaussian case, deviations from scaling for the susceptibility are very small.

We give estimates in tabular form for the critical temperatures and exponents, Table I. With the values of  $T_g$  in the table, the ratio  $T_g(\text{Gaussian})/T_g(\text{binomial})$  is in good agreement with Migdal-Kadanoff [15,16] and series [17] ratios. There appear to be no basic inconsistencies among the estimates from the diverse numerical techniques, and the values of Table I should be reliable. Clearly, in confirmation of conclusions drawn in [5,7], the exponents  $\eta$ ,  $z$ , and perhaps  $\nu$  appear to be significantly different for the two  $3d$  ISG systems. With the present values of  $T_g$  at hand together with the Binder cumulant values  $g_L(T_g)$  for the largest  $L$  in each system [4,6], the critical  $g_L$  values are  $0.69 \pm 0.01$  for the

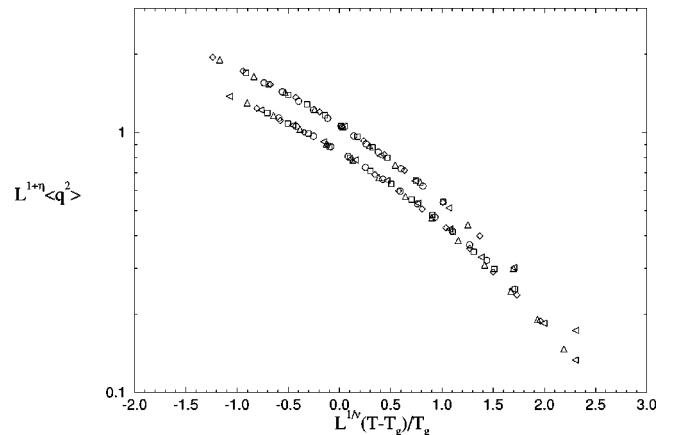


FIG. 12. Scaling plots of  $\langle q^2 \rangle$  for both the  $3d \pm J$  ISG and the  $3d$  Gaussian ISG model. The two scaling functions are clearly different.

binomial case and  $0.78 \pm 0.02$  for the Gaussian case. Again, this parameter, which should be universal for a given class of transitions, appears to change with the form of the interactions. Finally we can plot the scaling functions for  $\langle q^2 \rangle$  together, Fig. 12. It can be seen that the two scaling functions, which should be identical if universality were obeyed, are clearly different. The standard universality rules do not seem to hold for the critical exponent values of these ISG models.

#### ACKNOWLEDGMENTS

We are very grateful to N. Kawashima and A. P. Young and to E. Marinari, G. Parisi, and J. J. Ruiz-Lorenzo for sending us their high quality numerical data. We would like to thank A. Aharony, A. B. Harris, and J. Adler for very useful discussions. Our numerical simulations were carried out thanks to a time allocation from IDRIS (Institut du Développement des Ressources en Informatique Scientifique).

- 
- [1] J. C. Le Guillou and J. Zinn-Justin, Phys. Rev. Lett. **39**, 95 (1977); Phys. Rev. B **21**, 3976 (1980).
  - [2] R. Guida and J. Zinn-Justin, e-print cond-mat/9803240.
  - [3] A. T. Ogielski, Phys. Rev. B **32**, 7384 (1985).
  - [4] N. Kawashima and A. P. Young, Phys. Rev. B **53**, R484 (1996).
  - [5] L. W. Bernardi, S. Prakash, and I. A. Campbell, Phys. Rev. Lett. **77**, 2798 (1996).
  - [6] E. Marinari, G. Parisi, and J. J. Ruiz-Lorenzo, e-print cond-mat/9802211.
  - [7] L. W. Bernardi and I. A. Campbell, Phys. Rev. B **56**, 5271 (1997).
  - [8] R. N. Bhatt and A. P. Young, Phys. Rev. B **37**, 5606 (1988).
  - [9] H. G. Ballesteros, L. A. Fernández, V. Martin-Mayor, A. Muñoz Sudupe, G. Parisi, and J. J. Ruiz-Lorenzo, e-print cond-mat/9805125.
  - [10] K. K. Mon, Europhys. Lett. **34**, 399 (1996).
  - [11] D. A. Huse, Phys. Rev. B **40**, 304 (1989).
  - [12] H.K. Janssen, B. Schaub, and B. Schmittmann, Z. Phys. B **73**, 539 (1989).
  - [13] L. Klein, J. Adler, A. Aharony, A. B. Harris, and Y. Meir, Phys. Rev. B **43**, 11 249 (1991).
  - [14] J. Adler, Annu. Rev. Comput. Phys. **4**, 241 (1996).
  - [15] S. Prakash and I. A. Campbell, Physica A **235**, 507 (1997).
  - [16] E. Noguiera, S. Coutinho, F. D. Nobre, E. M. F. Curado, and J. R. L. de Almeida, Phys. Rev. E **55**, 3934 (1997).
  - [17] R. P. R. Singh and M. E. Fisher, J. Appl. Phys. **63**, 3994 (1988).